

MiR-141-3p regulates myogenic differentiation in C2C12 myoblasts via CFL2-YAP-mediated mechanotransduction

Mai Thi Nguyen & Wan Lee*

Department of Biochemistry, Dongguk University College of Medicine, Gyeongju 38066, Korea

Skeletal myogenesis is essential to keep muscle mass and integrity, and impaired myogenesis is closely related to the etiology of muscle wasting. Recently, miR-141-3p has been shown to be induced under various conditions associated with muscle wasting, such as aging, oxidative stress, and mitochondrial dysfunction. However, the functional significance and mechanism of miR-141-3p in myogenic differentiation have not been explored to date. In this study, we investigated the roles of miR-141-3p on CFL2 expression, proliferation, and myogenic differentiation in C2C12 myoblasts. MiR-141-3p appeared to target the 3'UTR of CFL2 directly and suppressed the expression of CFL2, an essential factor for actin filament (F-actin) dynamics. Transfection of miR-141-3p mimic in myoblasts increased F-actin formation and augmented nuclear Yes-associated protein (YAP), a key component of mechanotransduction. Furthermore, miR-141-3p mimic increased myoblast proliferation and promoted cell cycle progression throughout the S and G2/M phases. Consequently, miR-141-3p mimic led to significant suppressions of myogenic factors expression, such as MyoD, MyoG, and MyHC, and hindered the myogenic differentiation of myoblasts. Thus, this study reveals the crucial role of miR-141-3p in myogenic differentiation via CFL2-YAP-mediated mechanotransduction and provides implications of miRNA-mediated myogenic regulation in skeletal muscle homeostasis. [BMB Reports 2022; 55(2): 104-109]

INTRODUCTION

Skeletal muscle is a dynamic and plastic tissue essential for proper locomotion and metabolic functioning (1). Muscle wasting or atrophy is closely linked to various conditions associated with the inhibition of myogenesis, such as senescence, ER stress, oxidative stress, and mitochondrial dysfunction (2). Myogenesis

is a well-coordinated complex process and underlies myofiber formation for muscle development and regeneration (3). During myogenesis, satellite cells exit quiescence, rapidly proliferate until they exit the cell cycle, and then after the activations of myogenic factors, differentiate into myotubes (3). Over the past two decades, a growing body of research has increased our understanding of the critical roles played by miRNAs in myogenesis and their impacts on muscle homeostasis and wasting (4). However, the mechanisms whereby specific miRNAs regulate myogenic differentiation remain elucidated.

MicroRNAs (miRNAs) comprise a large family of endogenous short non-coding RNAs that suppress gene expressions by binding to the 3'UTRs of target mRNAs (5). Accumulating evidence has suggested that miRNAs are critical modulators of skeletal muscle proliferation, differentiation, and regeneration (6). MiR-141-3p, a member of the miR-200 family, has recently been considered an oncogenic miRNA because it facilitates tumorigenesis, metastasis, and resistance to chemotherapy by promoting cell proliferation, growth, and survival (7, 8). Interestingly, miR-141-3p has been reported to be upregulated during various conditions associated with muscle wasting, such as ER stress, oxidative stress, and mitochondrial dysfunction (9-11). Moreover, the expression of miRNA-141-3p was also increased in various cells during cellular senescence, which is associated with sarcopenia (9, 12, 13). These findings imply that miR-141-3p may be implicated in myogenesis and muscle homeostasis by regulating cell proliferation and growth. However, the role and significance of miR-141-3p in myogenic differentiation of progenitor cells have not been explored.

Based on the results of *in silico* miR-target prediction analysis, Cofilin 2 (CFL2) appears to be a potential target of miR-141-3p. CFL2 is a skeletal muscle-specific actin-binding protein that belongs to the actin depolymerizing factor (ADF)/cofilin family, which promotes the disassembly of filamentous actin (F-actin) (14). Many studies suggest that CFL2 is a vital player in the maintenance of muscle architecture by regulating actin filament dynamics in skeletal muscle (14). CFL2 knockout in mice proved lethal within seven days of birth due to skeletal muscle weakness, sarcomere structure disruption, and F-actin accumulations with a loss of actin depolymerization activity (15). Furthermore, CFL2 knockout developed progressive muscle degeneration with fiber size disproportion, sarcoplasmic protein aggregates, and mitochondrial abnormalities (16). Recently, we revealed that CFL2

*Corresponding author. Tel: +82-54-770-2409; Fax: +82-54-770-2447; E-mail: wanlee@dongguk.ac.kr

<https://doi.org/10.5483/BMBRep.2022.55.2.142>

Received 5 October 2021, Revised 8 November 2021,
Accepted 8 November 2021

Keywords: CFL2, Differentiation, Mechanotransduction, MiR-141-3p, Myogenesis

knockdown in myoblasts inhibited myogenic differentiation by promoting cell proliferation (17). In addition, CFL-mediated actin remodeling has been suggested to regulate cell proliferation and myogenic differentiation (18, 19). Although prior research has shown that CFL2 is required for skeletal muscle myogenesis, little is known about the miRNAs that regulate CFL2 and their significance in myogenic differentiation.

In this study, we investigated the role played by miR-141-3p on the regulation of CFL2 and myogenic differentiation in C2C12 myoblasts. Interestingly, miR-141-3p was found to suppress CFL2 expression by targeting the 3'UTR of CFL2. Furthermore, the role of miR-141-3p in myoblast proliferation, myogenic factor expression, and differentiation was shown in conjunction with mechanotransduction. Thus, this study suggests the crucial role of miR-141-3p in myogenic differentiation via the CFL2/F-actin/YAP axis and provided implications of miRNA-mediated actin dynamics as a myogenic regulatory mechanism.

RESULTS

MiR-141-3p directly targeted the 3'UTR of CFL2

We hypothesized that miR-141-3p might inhibit myogenic differentiation by suppressing CFL2. Therefore, we first investigated whether miR-141-3p directly targets and suppresses CFL2 expression in myoblasts. According to miRNA target prediction analysis using TargetScan and miRWalk, CFL2 is a potential target of miR-141-3p because the 3'UTR of CFL2 contains a tentative

binding site with a high affinity for the seed sequence of miR-141-3p (Fig. 1A). To confirm direct targeting of CFL2 3'UTR by miR-141-3p, the 3'UTR segment of CFL2 containing a tentative miR-141-3p binding site (wild-type; CFL2-wt) or mutated sequences (CFL2-mut) were cloned into pmirGLO luciferase reporter vector (Fig. 1B). As shown in Fig. 1C, co-transfection with miR-141-3p mimic decreased luciferase activity of the reporter containing a wild-type (CFL2-wt). In contrast, mutations on the miR-141-3p binding site (CFL2-mut) almost completely rescued the inhibitory effect of miR-141-3p in CFL2-wt, confirming direct binding between miR-141-3p and the 3'UTR of CFL2. Next, to examine whether miR-141-3p induction suppresses CFL2 expression in myoblasts, C2C12 myoblasts were transfected with scRNA control or miR-141-3p mimic, and then the expression of CFL2 was determined. As shown in Fig. 1D, transfection with miR-141-3p mimic significantly reduced the protein expression of CFL2 in C2C12 myoblasts as compared to scRNA. Moreover, the transcription of CFL2 was also suppressed slightly but significantly by miR-141-3p mimic as determined by RT-PCR and qRT-PCR (Fig. 1E). These results indicate that miR-141-3p regulates the expression of CFL2 by directly targeting CFL2 3'UTR.

MiR-141-3p increased F-actin formation and nuclear YAP

We previously reported that knockdown of CFL2 resulted in marked accumulation of F-actin in myoblasts (17). Since miR-141-3p targets CFL2 directly (Fig. 1), we next determined whether the ectopic expression of miR-141-3p could modulate the reorganization of F-actin. Although transfection with CFL2 siRNAs,

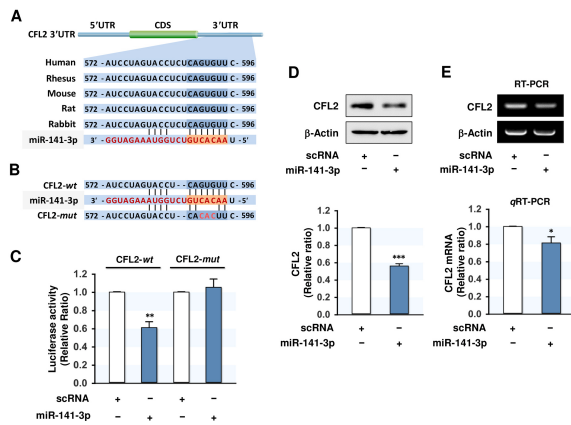


Fig. 1. MiR-141-3p repressed CFL2 by binding directly to CFL2 3' UTR. (A) A potential binding site for miR-141-3p on CFL2 3'UTR in various species. (B) The wild-type (CFL2-wt) and mutant (CFL2-mut) binding site on CFL2 3'UTR for miR-141-3p. (C) A pmirGLO vector containing CFL2-wt or CFL2-mut was co-transfected with scRNA or miR-141-3p mimic into C2C12 cells, and luciferase activities were analyzed. (D) CFL2 protein level was determined 48 h after transfection by immunoblotting. (E) CFL2 mRNA level was analyzed 24 h after transfection by RT-PCR (upper) and qRT-PCR (lower). All expression levels were normalized to the amount of β -Actin. The values are shown as the relative ratio where the intensity of normalized scRNA control was set to one. Results are presented as means \pm SEMs ($n > 3$). * $P < 0.05$; ** $P < 0.01$; *** $P < 0.001$ vs scRNA.

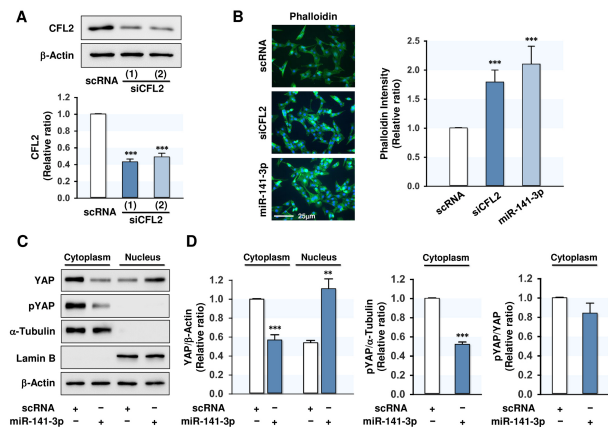


Fig. 2. MiR-141-3p increased F-actin formation and nuclear YAP levels. C2C12 myoblasts were transfected with 200 nM of scRNA, CFL2 siRNA (siCFL2) or miR-141-3p mimic (miR-141-3p). (A) After 24 h, CFL2 protein expressions were determined by immunoblotting. (B) Representative images of cells stained with FITC-conjugated phalloidin (green) and Hoechst 33342 (blue). Scale bar: 25 μ m. (C) Immunoblots of YAP and phospho-YAP (pYAP) in the cytoplasm and nuclear fractions. (D) Quantitative analysis of immunoblots. The values shown are relative ratios versus scRNA controls. Results are presented as means \pm SEMs ($n > 3$). ** $P < 0.01$; *** $P < 0.001$ vs scRNA.

namely siCFL2(1) and siCFL2(2), suppressed CFL2 protein expression by ~55% as compared with scRNA control (Fig. 2A), we found that siCFL2(2) had a slight cytotoxic effect at a dose of 200 nM. Therefore, we used siCFL2(1) for the subsequent experiments. Transfection with miR-141-3p mimic markedly increased (>200-fold) the cellular level of miR-141-3p (data not shown). Remarkably, transfection with miR-141-3p mimic or siCFL2 elevated F-actin accumulation (Fig. 2B). Given that overall actin levels remained constant during the differentiation period in all groups, these F-actin increases appeared to be the consequence of impaired actin depolymerization. Therefore, it is suggested that miR-141-3p restricts actin dynamics and augments F-actin by suppressing CFL2 in myoblasts. F-actin has been shown to stimulate the nuclear translocation of transcriptional coactivator YAP, which modulates mechanotransduction in the Hippo signaling pathway and activates proliferative transcriptional programs (20). To determine the effect of miR-141-3p on YAP translocation, we next evaluated the phosphorylation (Y357) and nuclear localization of YAP in myoblasts. Transfection with miR-141-3p mimic dramatically reduced YAP phosphorylation in the cytoplasm and subsequently redistributed YAP to the nucleus from the cytosol (Fig. 2C, D). Thus, it appeared that the effect of miR-141-3p on the nuclear translocation of YAP was mainly ascribed to CFL2 suppression.

MiR-141-3p promoted cell proliferation and cell cycle progression

Previously, CFL2 deficiency was shown to hinder myogenic differentiation by promoting cell proliferation and cell cycle progression (17). Since miR-141-3p mimic suppressed CFL2 expression in myoblasts, we examined the effect of miR-141-3p on myoblast proliferation and cell cycle progression. EdU incorporation analysis showed that CFL2 siRNA significantly increased the proportion of EdU-positive cells compared with scRNA (Fig. 3A, B), which demonstrated CFL2 depletion increased myoblast proliferation. As expected, transfection with miR-141-3p mimic also drastically increased EdU-incorporated myoblasts, whereas co-transfection with anti-miR-141 rescued EdU incorporation similar to those observed after scRNA transfection (Fig. 3A, B), indicating that miR-141-3p enhanced myoblast proliferation. We next analyzed the transcriptions of proliferating cell nuclear antigen (PCNA) and CCND1, which are associated with cell proliferation and cell cycle progression as YAP target genes. qRT-PCR results showed that the mRNA levels of PCNA and CCND1 were significantly upregulated in myoblasts transfected with miR-141-3p mimic (Fig. 3C). In addition, we determined the effect of miR-141-3p on cell cycle phases by flow cytometry. The transfection of miR-141-3p mimic decreased the proportion of cells in the G0/G1 phase but increased in the S and G2/M phases (Fig. 3D). Thus, the induction of

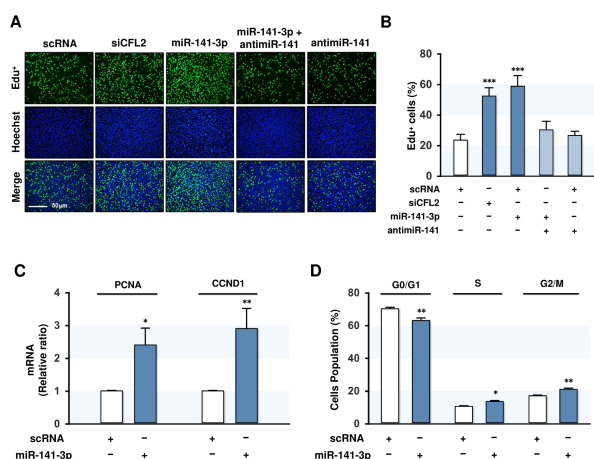


Fig. 3. MiR-141-3p promoted myoblast proliferation and cell cycle progression. C2C12 myoblasts were transfected with 200 nM of scRNA, siCFL2, miR-141-3p mimic (miR-141-3p), or anti-miR-141. (A) Representative images of EdU (green) and Hoechst 33342 (blue) staining. Scale bar: 50 μ m. (B) Percentages of EdU-positive cells were determined using ImageJ software. (C) qRT-PCR of PCNA and CCND1. Expression levels were normalized versus U6. (D) Flow cytometry after transfection with scRNA or miR-141-3p mimic. Values are presented as relative ratios versus scRNA controls. Results are expressed as means \pm SEMs ($n > 3$). * $P < 0.05$; ** $P < 0.01$; *** $P < 0.001$ vs scRNA.

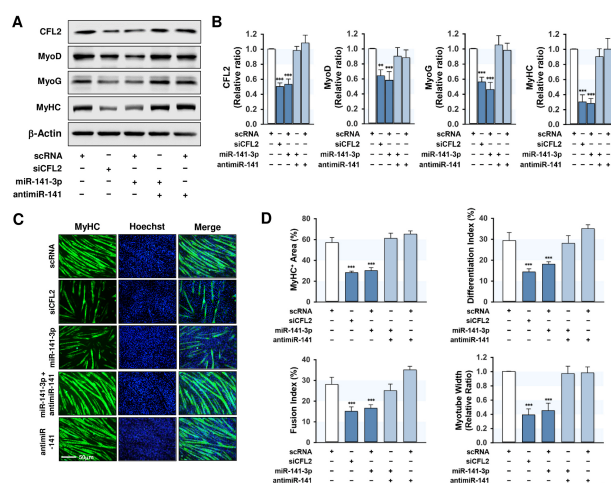


Fig. 4. MiR-141-3p suppressed the expressions of myogenic factors and impaired myogenic differentiation. 200 nM of scRNA control, siCFL2, miR-141-3p mimic (miR-141-3p), or anti-miR-141 were transfected into C2C12 cells. (A) Immunoblots were obtained after three days of differentiation. (B) Quantitative analysis of the protein expressions for CFL2 and myogenic factors. Protein levels were normalized versus β -actin. (C) After five days of differentiation, MyHC (green)-positive myotubes were obtained by immunofluorescence staining, and nuclei were counterstained with Hoechst (blue). Scale bar: 50 μ m. (D) MyHC-positive areas, differentiation indices, fusion indices, and myotube widths were determined as described in the Methods. Results are presented as means \pm SEMs ($n > 3$). *** $P < 0.001$ vs scRNA.

miR-141-3p in myoblasts was found to promote cell proliferation and cell cycle progression.

MiR-141-3p inhibited the expressions of myogenic factors

We further investigated whether the induction of miR-141-3p suppresses the expressions of myogenic factors. C2C12 cells transfected with scRNA, siCFL2, miR-141-3p mimic, or anti-miR-141-3p were cultured for three days in differentiation medium, and then the protein levels of myogenic factors were analyzed (Fig. 4A, B). Transfection with siCFL2 reduced CFL2 level by about 55% versus scRNA control and significantly suppressed the expressions of myogenic factors, such as MyoD, MyoG, and MyHC, in myoblasts. Interestingly, miR-141-3p mimic transfection also suppressed the expression of CFL2 markedly and reduced myogenic factors' levels compared with scRNA controls. Furthermore, co-transfection with miR-141-3p and anti-miR-141 rescued myogenic factor levels similar to scRNA transfection (Fig. 4A, B). The ineffectiveness of anti-miR-141 alone may be ascribed to the low endogenous level of miR-141-3p and the abundance of CFL2 in C2C12 myoblasts. Because CFL2 knockdown inhibits myogenic differentiation and there are no putative miR-141-3p binding sites on the 3'UTRs of MyoD, MyoG, and MyHC, the suppression of myogenic factors by miR-141-3p mimic is attributed to CFL2 reduction. Thus, these findings indicate that miR-141-3p plays a critical role in the regulation of myogenic factors in C2C12 myoblasts.

MiR-141-3p impaired the myogenic differentiation of myoblasts

Since miR-141-3p mimic increased cell proliferation and suppressed the expressions of myogenic factors, we examined whether miR-141-3p inhibits the myogenic differentiation of C2C12 myoblasts. Cells were transfected with scRNA, siCFL2, miR-141-3p mimic, or anti-miR-141-3p and then differentiated for five days. Myogenic differentiation was determined quantitatively by immunocytochemistry using MyHC antibody and Hoechst stain (Fig. 4C, D). The knockdown of CFL2 dramatically inhibited myotube formation. In addition, the percentage area of MyHC-positive cells, differentiation index, fusion index, and myotube width indicated that CFL2 downregulation resulted in impaired myogenic differentiation (Fig. 4C, D). Similarly, transfection with miR-141-3p mimic instead of siCFL2 inhibited the differentiation of myoblasts as assessed by immunocytochemistry and differentiation analysis. Furthermore, co-transfection with anti-miR-141-3p almost completely abolished the inhibitions of myogenic differentiation and myotube formation mediated by miR-141-3p mimic (Fig. 4C, D). Collectively, these results suggest that miR-141-3p regulates myogenic factors and differentiation in myoblasts.

DISCUSSION

MiRNAs have been implicated in myogenesis and muscle homeostasis by variously regulating proliferation, the cell cycle, and differentiation (6). This study unveiled the crucial roles of miR-141-3p on CFL2 expression, cell proliferation, and myo-

genic differentiation. The following are the key contributions this study makes to current understanding: (i) miR-141-3p suppressed the expression of CFL2 by directly targeting the 3'UTR of CFL2. (ii) Ectopic expression of miR-141-3p mimic increased F-actin formation and augmented the nuclear accumulation of YAP in myoblasts. (iii) Transfection of miR-141-3p mimic increased cell proliferation and promoted cell cycle progression. (iv) MiR-141-3p mimic markedly reduced the levels of myogenic factors, such as MyoD, MyoG, and MyHC, and hindered the myogenic differentiation.

Hsa-miR-141-3p is a member of the miR-200 family, which in vertebrates is consisted of five miRNAs viz miR-141, 200a, 200b, 200c, and 429 (8). Although the significance of miR-141-3p in myogenesis has not been previously explored, miRNA-141-3p has been reported to be induced in a variety of conditions related to muscle wasting, including oxidative stress (10), mitochondrial dysfunction (11), and senescence (9, 12, 13). Hence, we hypothesize that dysregulation of miR-141-3p contributes substantially to impaired myogenesis and muscle wasting. Notably, we found miR-141-3p mimic stimulated cell proliferation and cell cycle progression in myoblasts and subsequently suppressed myogenic differentiation (Figs. 3 and 4). Proliferation and differentiation of myoblasts have long been established to be inversely associated during myogenesis, and thus, arrest in proliferation is a prerequisite of myogenic differentiation and myotube formation (3). Accordingly, the promotion of proliferation and the cell cycle by miR-141-3p is intimately connected to the impaired myogenic differentiation in myoblasts. Recent research on various cancers has supported the effect of miR-141-3p on cell proliferation, apoptosis, and the cell cycle. MiR-141-3p has been reported to be upregulated in various malignancies, such as colorectal cancer, lung cancer, prostate cancer, and cervical cancer (7). Moreover, miR-141-3p overexpression increased cell proliferation, while miR-141-3p knockdown suppressed the proliferation of various cell types (21-24). In addition, this study showed that miR-141-3p stimulated the gene expressions of PCNA and CCND1, which are target genes of YAP and related to cell cycle progression. This result is in line with previous reports that miR-141-3p upregulates PCNA in the intestinal tissues of mice (25) and CCND1 in nasopharyngeal carcinoma (26). Therefore, the inhibition of myogenic differentiation by miR-141-3p mimic may be primarily ascribed to increased myoblast proliferation and cell cycle progression.

Then what is the underlying molecular mechanism whereby miR-141-3p promotes myoblast proliferation and cell cycle progression? One key finding of this study is that miR-141-3p mimic transfection directly suppressed CFL2 expression and increased F-actin in myoblasts (Fig. 2). CFL2 regulates actin remodeling by cleaving F-actin and thus, plays an essential role in cytoskeleton dynamics (19). Interestingly, actin dynamics has been suggested to be a key regulator of YAP in the Hippo signaling pathway (27). Previously, F-actin was shown to inhibit the phosphorylation of YAP and TAZ, which increased their nuclear translocations and led to cell proliferation as a mechanotransduction

mechanism (20). Furthermore, F-actin severing proteins, such as CFLs and Gelsolin, function as negative regulators of YAP and TAZ by increasing their phosphorylations (18). Thus, CFL-mediated actin remodeling is closely linked to the regulation of cell proliferation via the nuclear translocation of YAP (18, 19). A previous study showed that CFL2 knockdown augmented F-actin formation, promoted cell cycle progression, and stimulated myoblast proliferation (17). Similarly, Torrini *et al.* demonstrated that depletion of CFL2 in cardiomyocytes augmented F-actin level and activated YAP (28). In addition, treatment with cytochalasin D, a potent inhibitor of actin polymerization, prevented the nuclear translocation of YAP, while treatment with jasplakinolide, an F-actin inducer, increased this translocation (28).

In conclusion, this study demonstrates that miR-141-3p regulates myogenic differentiation by inhibiting CFL2 expression, implying that CFL2-YAP-mediated mechanotransduction is a critical component of the myogenic regulation mechanism. Thus, miR-141-3p may be a critical mediator in the relationship between mechanotransduction and myogenic differentiation, allowing for the development of effective diagnostic and therapeutic strategies for muscle wasting and atrophy.

MATERIALS AND METHODS

Cell culture

C2C12 cells, a murine myoblast cell line, were cultured in a growth medium (DMEM containing 10% fetal bovine serum and 1% penicillin/streptomycin) and induced myogenic differentiation as previously described (17). Unless otherwise stated, all reagents and materials were purchased from Sigma-Aldrich.

Cell transfection

CFL2 siRNA (siCFL2), miR-141-3p mimic, anti-miR-141 (an inhibitor of miR-141-3p), or scrambled control RNA (scRNA) (Genolution, Seoul, Korea) were transfected into C2C12 myoblasts at 200 nM using Lipofectamine 2000 (Invitrogen). Oligonucleotide sequences are shown in Supplementary Table 1.

RNA extraction and real-time quantitative PCR

Total RNA from C2C12 cells was extracted using Qiazol (Qiagen) and purified with a miRNeasy Mini Kit (Qiagen). cDNAs were synthesized using a miScript II RT Kit (Qiagen). SYBR Green I (Promega) was used for qRT-PCR in a LightCycler 480 (Roche Applied Science). All primer sequences and reaction conditions are shown in Supplementary Table 2.

Dual-luciferase reporter assay

Wild-type *CFL2* 3'UTR was synthesized by RT-PCR and inserted into the pmirGLO vector (Promega) using the primer sets described in Supplementary Table 2. Mutant *CFL2* 3'UTR was generated by site-directed mutagenesis using the primer set described in Supplementary Table 2. Dual-luciferase reporter gene assays were performed 24 h after transfection, as described (29).

Immunoblot analysis

Total protein was extracted using a lysis buffer, which consisted of 2% Triton X-100 and 0.1% phosphatase inhibitor cocktail (Sigma) in PBS, and lysates were dissolved in Laemmli solution (30). For subcellular protein fractionations, the NE-PER nuclear and cytoplasmic extraction reagents (Sigma) were used. Immunoblotting was conducted using specific antibodies described in Supplementary Table 3. Band intensities were determined by a Fusion Solo (Paris, France).

Immunofluorescence analysis

After differentiation, C2C12 myoblasts were fixed, permeabilized, and visualized with MyHC antibodies, Alexa 488-conjugated goat anti-mouse antibody (Invitrogen), and Hoechst 33342 (Invitrogen), as described previously (17, 31). Differentiation indices were calculated by expressing numbers of nuclei in MyHC-positive myotubes as percentages of total numbers of nuclei in fields, and fusion indices were calculated by expressing numbers of myotubes with three or more nuclei as percentages of total numbers of nuclei. MyHC-positive areas, numbers of myotubes, and myotube widths were measured using ImageJ Software. All experiments were conducted at least three times using at least five randomly selected fields per experiment.

F-actin analysis, cell proliferation assays, and flow cytometry analysis

For F-actin staining, cells were fixed, permeabilized, and incubated with FITC-conjugated phalloidin, as described previously (17). Cell proliferation was determined using the Click-iT™ EdU Cell Proliferation Kit (Invitrogen) according to the previous study (17). For flow cytometry analysis, Cell Cycle kit (C03551, Beckman Coulter, USA) was used in a CytoFLEX (Beckman Coulter, USA).

miRNA target gene predictions and statistical analysis

The potential binding site of miR-141-3p on the *CFL2* 3'UTR was analyzed using publicly available bioinformatics software (TargetScan: www.targetscan.org, miRWalk: mirwalk.umm.uni-heidelberg.de). Results are presented as the means ± standard errors of at least three independent experiments. Statistical significance between groups was determined using the Student's *t*-test.

ACKNOWLEDGEMENTS

This study was supported by the National Research Foundation of Korea (NRF) funded by the Korean government (Grant no. NRF-2019R1F1A1040858).

CONFLICTS OF INTEREST

The authors have no conflicting interests.

REFERENCES

1. Frontera WR and Ochala J (2015) Skeletal muscle: a brief review of structure and function. *Calcif Tissue Int* 96, 183-195
2. Sartori R, Romanello V and Sandri M (2021) Mechanisms of muscle atrophy and hypertrophy: implications in health and disease. *Nat Commun* 12, 330
3. Chal J and Pourquie O (2017) Making muscle: skeletal myogenesis in vivo and in vitro. *Development* 144, 2104-2122
4. Mok GF, Lozano-Velasco E and Munsterberg A (2017) microRNAs in skeletal muscle development. *Semin Cell Dev Biol* 72, 67-76
5. Krol J, Loedige I and Filipowicz W (2010) The widespread regulation of microRNA biogenesis, function and decay. *Nat Rev Genet* 11, 597-610
6. Sannicandro AJ, Soriano-Arroquia A and Goljanek-Whysall K (2019) Micro(RNA)-managing muscle wasting. *J Appl Physiol* 127, 619-632
7. Gao Y, Feng B, Han S et al (2016) The roles of microRNA-141 in human cancers: from diagnosis to treatment. *Cell Physiol Biochem* 38, 427-448
8. Senfter D, Madlener S, Krupitza G et al (2016) The microRNA-200 family: still much to discover. *Biomol Concepts* 7, 311-319
9. Fariyike B, Singleton Q, Hunter M et al (2019) Role of microRNA-141 in the aging musculoskeletal system: a current overview. *Mech Ageing Dev* 178, 9-15
10. Zaccagnini G, Martelli F, Magenta A et al (2007) p66(ShcA) and oxidative stress modulate myogenic differentiation and skeletal muscle regeneration after hind limb ischemia. *J Biol Chem* 282, 31453-31459
11. Ji J, Qin Y, Ren J et al (2015) Mitochondria-related miR-141-3p contributes to mitochondrial dysfunction in HFD-induced obesity by inhibiting PTEN. *Sci Rep* 5, 16262
12. Yu KR, Lee S, Jung JW et al (2013) MicroRNA-141-3p plays a role in human mesenchymal stem cell aging by directly targeting ZMPSTE24. *J Cell Sci* 126, 5422-5431
13. Periyasamy-Thandavan S, Burke J, Mendhe B et al (2019) MicroRNA-141-3p negatively modulates SDF-1 expression in age-dependent pathophysiology of human and murine bone marrow stromal cells. *J Gerontol A Biol Sci Med Sci* 74, 1368-1374
14. Kanellos G and Frame MC (2016) Cellular functions of the ADF/cofilin family at a glance. *J Cell Sci* 129, 3211-3218
15. Agrawal PB, Joshi M, Savic T et al (2012) Normal myofibrillar development followed by progressive sarcomeric disruption with actin accumulations in a mouse Cfl2 knockout demonstrates requirement of cofilin-2 for muscle maintenance. *Hum Mol Genet* 21, 2341-2356
16. Gurniak CB, Chevessier F, Jokwitz M et al (2014) Severe protein aggregate myopathy in a knockout mouse model points to an essential role of cofilin2 in sarcomeric actin exchange and muscle maintenance. *Eur J Cell Biol* 93, 252-266
17. Nguyen MT, Min KH, Kim D et al (2020) CFL2 is an essential mediator for myogenic differentiation in C2C12 myoblasts. *Biochem Biophys Res Commun* 533, 710-716
18. Aragona M, Panciera T, Manfrin A et al (2013) A mechanical checkpoint controls multicellular growth through YAP/TAZ regulation by actin-processing factors. *Cell* 154, 1047-1059
19. Bernstein BW and Bamberg JR (2010) ADF/cofilin: a functional node in cell biology. *Trends Cell Biol* 20, 187-195
20. Dupont S (2016) Role of YAP/TAZ in cell-matrix adhesion-mediated signalling and mechanotransduction. *Exp Cell Res* 343, 42-53
21. Mei Z, He Y, Feng J et al (2014) MicroRNA-141 promotes the proliferation of non-small cell lung cancer cells by regulating expression of PHLPP1 and PHLPP2. *FEBS Lett* 588, 3055-3061
22. Li JH, Zhang Z, Du MZ et al (2018) microRNA-141-3p fosters the growth, invasion, and tumorigenesis of cervical cancer cells by targeting FOXA2. *Arch Biochem Biophys* 657, 23-30
23. Guo D, Jiang H, Chen Y et al (2018) Elevated microRNA-141-3p in placenta of non-diabetic macrosomia regulate trophoblast proliferation. *EBioMedicine* 38, 154-161
24. Liu Y, Zhao R, Wang H et al (2016) miR-141 is involved in BRD7-mediated cell proliferation and tumor formation through suppression of the PTEN/AKT pathway in nasopharyngeal carcinoma. *Cell Death Dis* 7, e2156
25. Qian WH, Liu YY, Li X et al (2019) MicroRNA-141 ameliorates alcoholic hepatitis-induced intestinal injury and intestinal endotoxemia partially via a TLR4-dependent mechanism. *Int J Mol Med* 44, 569-581
26. Zhang L, Deng T, Li X et al (2010) microRNA-141 is involved in a nasopharyngeal carcinoma-related genes network. *Carcinogenesis* 31, 559-566
27. Mendez MG and Janmey PA (2012) Transcription factor regulation by mechanical stress. *Int J Biochem Cell Biol* 44, 728-732
28. Torrini C, Cubero RJ, Dirx E et al (2019) Common regulatory pathways mediate activity of microRNAs inducing cardiomyocyte proliferation. *Cell Rep* 27, 2759-2771 e2755
29. Yang WM, Jeong HJ, Park SW et al (2015) Obesity-induced miR-15b is linked causally to the development of insulin resistance through the repression of the insulin receptor in hepatocytes. *Mol Nutr Food Res* 59, 2303-2314
30. Ryu HS, Park SY, Ma D et al (2011) The induction of microRNA targeting IRS-1 is involved in the development of insulin resistance under conditions of mitochondrial dysfunction in hepatocytes. *PLoS One* 6, e17343
31. Nguyen MT, Min KH and Lee W (2020) MiR-183-5p induced by saturated fatty acids regulates the myogenic differentiation by directly targeting FHL1 in C2C12 myoblasts. *BMB Rep* 53, 605-610